

# Analyzing and Mitigating the Impacts of GMD and EMP Events on the Electrical Grid with PowerModelsGMD.jl

Adam Mate <sup>1</sup>, Arthur K. Barnes <sup>1</sup>, Russell W. Bent <sup>1</sup>, and Eduardo Cotilla-Sanchez <sup>2</sup>

**Abstract**—Geomagnetic disturbances and E3 high-altitude electromagnetic pulse events pose a substantial threat to the electrical grid by adversely impacting and damaging high-voltage transmission networks and equipment. To evaluate the risks and mitigate the potential effects of these hazards, this work proposes PowerModelsGMD.jl (abbr. PMsGMD). PMsGMD is an open-source Julia package that solves for quasi-dc line flow and ac power flow problems in a system subjected to geomagnetically induced currents. Unlike commercially available software solutions, it is extensible and applicable to a variety of problems. The flexibility of this framework is demonstrated by applying it to the problem of identifying mitigation strategies via line switching for a time-extended transformer heating problem.

An overview of PMsGMD is presented in this paper: introduction to its design, validation of its implementation, demonstration of its performance and effectiveness, and a description of how it may be applied to aid system-operation decisions.

**Index Terms**—power system analysis, geomagnetic disturbance, electromagnetic pulse, optimal power flow, Julia, open-source.

## I. INTRODUCTION

High-impact low-frequency (abbr. HILF) events are the greatest threat to the continuous and reliable operation of our energy infrastructures. Such events have the potential to cause unpredictable system-wide disruptions and long-term damage in the electrical grid, a key component of the critical infrastructures. Geomagnetic disturbances (abbr. GMDs) and high-altitude electromagnetic pulse (abbr. HEMP) events are among these extreme hazards [1], [2].

GMDs are caused by intense solar activity: charged and magnetized particles are blown away from the Sun during severe space weather, which then interact with and disrupt the Earth's magnetic field causing rapid changes in its configuration. These disturbances are mainly driven by large solar flares and associated coronal mass ejections during solar maximums, and by co-rotating interaction regions (high-speed solar winds) during solar minimums [3]–[5].

HEMP events are caused by nuclear explosions detonated high up in the atmosphere. These are series of electromagnetic waveforms, covering times from nanoseconds to hundreds of seconds, that propagate to the Earth's surface. Three main waveforms are generated during a detonation, among which the E3 late-time waveform produces electric fields with comparable time scales and area coverage as those of geomagnetic storms. Even though GMDs tend to have higher energy,

E3 HEMP events generate high enough peak field levels that makes them comparable to severe GMD events in terms of impact and caused damage [4], [6].

Both GMD and E3 HEMP events pose a risk to the electrical grid by generating geomagnetically induced currents (abbr. GICs), quasi-dc currents that appear in the conductive infrastructure and flow into the high-voltage network through the neutrals of power transformers [4]–[7]. GICs may adversely impact transmission networks and equipment as they have the potential to induce harmonics by causing half-cycle saturation in transformers. Harmonics may lead to the misoperation of protective devices, causing tripping of over-current relays. Premature aging, lasting damage, or complete failure of large high-voltage transformers due to overheating and thermal degradation is also a great threat. Increased reactive power consumption, caused by the circulating GICs in the system, may lead to the loss of reactive power support and to voltage collapses. In the worst case, widespread infrastructure damage and tripping of transmission lines may result in cascading failures and extended power disruptions [8]–[12].

Understanding the danger that power systems face is critically important. This paper presents an overview of PowerModelsGMD.jl<sup>1</sup> (abbr. PMsGMD), a free and open-source package for power system simulation, which was specifically designed to evaluate the risks and mitigate the impacts of the above mentioned hazards. The PMsGMD framework is implemented in Julia [13], a high-level just-in-time compiled programming language designed specifically for scientific computing. It is an extension to the PowerModels.jl (abbr. PMs) platform [14], a Julia/JuMP package for solving and evaluating steady-state power network optimization problems. JuMP [15] is a package for mathematical programming in Julia that specifies problems with algebraic constraints.

The key contributions of this paper include:

- An extensible, open-source software for modeling GICs in power systems.
- The first time-extended model of GIC that includes detrimental effects on transformers and that is appropriate for use in a mitigation optimization setting.
- A detailed discussion on modeling requirements for GIC calculations.

The remainder of this paper is organized as follows: A review of the PMsGMD package and background of key problem formulations are provided in Section II; it gives context to this work and explains design goals. Section III presents the implemented steady-state formulations, and Section IV

<sup>1</sup> The authors are with the Advanced Network Science Initiative at Los Alamos National Laboratory (LANL ANSI), Los Alamos, NM 87544 USA. Email:{amate, abarnes, rbent}@lanl.gov.

<sup>2</sup> The author is with the School of Electrical Engineering and Computer Science, Oregon State University, Corvallis, OR 97331 USA. Email:{ecs}@oregonstate.edu.

LA-UR-19-29623. Approved for public release; distribution is unlimited.

<sup>1</sup><https://github.com/lanl-ansi/PowerModelsGMD.jl>

describes the specifications of the time-extended GIC mitigation problem. Section V and VI validates the implementations and provides a practical example of how this framework can be used both in planning and operations environments. Section VII finishes with a few concluding remarks.

## II. PROBLEM FORMULATIONS

### A. Context of PMsGMD

The Julia programming language [13] is a high-level, high-performance, flexible dynamic language, which is appropriate for technical computing, with performance comparable to traditional statically-typed languages. Julia has many free and open-source packages available to provide specific toolkits and capabilities for diverse applications.

PMs [14] is a package for power system simulation: it provides a flexible platform for implementing and solving a wide range of steady-state network optimization and analysis problems; among others, it includes implementations of power flow (abbr. PF), optimal power flow (abbr. OPF), and optimal transmission switching (abbr. OTS) problem specifications. It relies on JuMP [15], which provides an ideal modeling layer for the wide range of optimization problems that arise in power systems research. The use of at least one solver is required; e.g., Ipopt [16] a fast and scalable solver for non-convex non-linear optimization. Commercial solvers such as Gurobi [17] and CPLEX [18] are supported as well.

In recent years PMs has emerged and filled a gap between ad-hoc research code and commercial tools such as PSS<sup>®</sup>E and PowerWorld<sup>®</sup> Simulator. It is similar to the open-source MATPOWER package [19] that is widely used in the academic environment to conduct research; however, dependence on the MATLAB<sup>®</sup> environment, licensing challenges for parallel calculations in a computing cluster, and difficulty in creating extensions present great limitations. There have been efforts to improve GIC modeling and include related analysis in power system simulation [20]–[24]. A number of free and commercially available software solutions exist – MATGMD [25], PowerWorld<sup>®</sup>'s GIC add-on [26], and PSS<sup>®</sup>E's GIC module [27] – however, these all are focused on modeling and analysis with often unverifiable and non-customizable capabilities. The PMsGMD package presented here builds on the PMs platform and provides an accessible and easy-to-handle framework to both analyze and mitigate the impacts of GMD and E3 HEMP events on electrical grids.

PMsGMD solves for quasi-dc line flow and ac power flow on a network subjected to GICs. It solves for mitigation strategies by treating the transformer overheating problem as an optimal transmission switching problem. Due to its open-source nature, it is easy to verify and customize its operation in order to best fit the application circumstances. Due to its speed and reliability, it is suitable to be a key component of toolkits (such as [28]) that monitor GMD manifestations in real-time, that predict GICs on the electrical grid, that assess risk, that enhance grid resilience by providing aid to system-operators, and that recommend modifications in the network configuration. Consequently, PMsGMD is equally useful for both research and industry application.

### B. Input File Format

PMsGMD uses several extensions to the PMs data format [14] to provide input for its problem formulations. For generality, it uses a separate dc network defined by *gmd\_bus* and *gmd\_branch* tables. To correctly calculate the increased reactive power consumption of each transformer, the *branch\_gmd* table adds all winding configuration related data; furthermore, the *branch\_thermal* table adds thermal data necessary to determine the temperature changes in transformers. The *bus\_gmd* table includes the latitude and longitude of buses in the ac network for use in distributionally robust optimization [29] or for convenience in plotting the system.

The description of B4GIC [30], an included four-bus test case is presented below to demonstrate the use of the PMs-GMD data format and introduce each input field. Some fields and descriptions are abbreviated due to space constraints; transformer is abbreviated as xfmr.

#### 1) GMD Bus Data Table: Table I.

*parent*: index of corresponding ac network bus  
*status*: binary value that defines the status of bus  
*g\_gnd*: admittance to ground [S]  
*name*: a descriptive name for the bus

TABLE I  
MPC.GMD\_BUS

<i>parent</i>	<i>status</i>	<i>g_gnd</i>	<i>name</i>
1	1	5	'dc_sub1'
2	1	5	'dc_sub2'
1	1	0	'dc_bus1'
2	1	0	'dc_bus2'
3	1	0	'dc_bus3'
4	1	0	'dc_bus4'

#### 2) GMD Branch Data Table: Table II.

*f\_bus*: 'from' bus in the gmd bus table  
*t\_bus*: 'to' bus in the gmd bus table  
*index*: index of corresponding ac network branch  
*status*: binary value that defines the status of branch  
*br\_r*: branch resistance [ $\Omega$ ]  
*br\_v*: induced quasi-dc voltage [V]  
*len\_km*: length of branch [km]  
*name*: a descriptive name for the branch

#### 3) Branch GMD Data Table: Table III.

*hi\_bus*: index of high-side ac network bus  
*lo\_bus*: index of low-side ac network bus  
*gmd\_br\_hi*: index of gmd branch corresponding to high-side winding (two-winding xfmrs)  
*gmd\_br\_lo*: index of gmd branch corresponding to low-side winding (two-winding xfmrs)  
*gmd\_k*: scaling factor to calculate reactive power consumption as a function of effective winding current [p.u.]

TABLE II  
MPC.GMD\_BRANCH

<i>f_bus</i>	<i>t_bus</i>	<i>parent</i>	<i>status</i>	<i>br_r</i>	<i>br_v</i>	<i>len_km</i>	<i>name</i>
3	1	1	1	0.1	0	0	'dc_xf1_hi'
3	4	2	1	1.001	170.788	170.788	'dc_br1'
4	2	3	1	0.1	0	0	'dc_xf2_hi'

TABLE III  
MPC.BRANCH\_GMD

<i>hi_bus</i>	<i>lo_bus</i>	<i>gmd_br_hi</i>	<i>gmd_br_lo</i>	<i>gmd_k</i>	<i>gmd_br_se</i>	<i>gmd_br_co</i>	<i>baseMVA</i>	<i>dispatch</i>	<i>type</i>	<i>config</i>
1	3	1	-1	1.793	-1	-1	100	1	'xfmr'	'gwyedelta'
1	2	-1	-1	-1	-1	-1	-1	1	'line'	'none'
2	4	3	-1	1.793	-1	-1	100	1	'xfmr'	'gwyedelta'

TABLE IV  
MPC.BRANCH\_THERMAL

<i>xfmr</i>	<i>temp_amb</i>	<i>hs_inst_lim</i>	<i>hs_avg_lim</i>	<i>hsRated</i>	<i>to_time_c</i>	<i>toRated</i>	<i>to_init</i>	<i>to_inited</i>	<i>hs_coeff</i>
1	25	280	240	150	71	75	0	1	0.63
0	-1	-1	-1	-1	-1	-1	-1	-1	-1
1	25	280	240	150	71	75	0	1	0.63

- gmd\_br\_se*: index of gmd branch corresponding to series winding (auto-xfmrs)  
*gmd\_br\_co*: index of gmd branch corresponding to common winding (auto-xfmrs)  
*baseMVA*: [MVA] base of xfmr  
*type*: type of branch – 'xfmr' / 'transformer' or 'line' or 'series\_cap'  
*config*: winding configuration of transformer

TABLE V  
MPC.BUS\_GMD

<i>lat</i>	<i>lon</i>
40	-89
40	-87
40	-89
40	-87

#### 4) Branch Thermal Data Table: Table IV.

- xfmr*: binary value that defines if branch is an 'xfmr' or not  
*temp\_amb*: ambient temperature of xfmr [°C]  
*hs\_inst\_lim*: 1-hour hot-spot temp. limit of xfmr [°C]  
*hs\_avg\_lim*: 8-hour hot-spot temp. limit of xfmr [°C]  
*hsRated*: hot-spot temperature-rise of xfmr at rated power [°C]  
*to\_time\_c*: top-oil temperature-rise time-constant of xfmr [min]  
*toRated*: top-oil temperature-rise of xfmr at rated power [°C]  
*to\_init*: initial top-oil temperature of xfmr [°C]  
*to\_inited*: binary value that defines the initial top-oil temperature of xfmr: 1 with *to\_init* value, 0 with steady-state value  
*hs\_coeff*: relationship of hot-spot temperature rise to  $I_{eff}$  [°C/A]

#### 5) Bus GMD Data Table: Table V.

- lat*: latitude coordinate of ac network bus and corresponding dc network bus  
*lon*: longitude coordinate of ac network bus and corresponding dc network bus

The related fields of Branch GMD Data (Table III) and Branch Thermal Data (Table IV) tables are set to (−1) when a system component is not a transformer. PMsGMD is able to model both fixed (spatially uniform) and realistic (non-uniform) electric fields as it does not model line coupling.

#### C. Modeling GIC Impact

The goal of modeling is to accurately simulate GICs and determine the exact threat at any particular place and time in a power system. As the level of detail required to model a system is more than what is needed in a traditional positive-sequence simulation, it is a complex task [22]. GICs are dependent on system characteristics (geographical location of substations, resistance of system components, characteristics of transformers), geomagnetic source fields (amplitude, frequency content, spatial characteristics), and the Earth conductivity structure (modeling method, substation grounding resistance, influence on geo-electric fields); all these need to be considered in the modeling process. The greatest challenge is the availability of data; verifiable information on the threat and detailed description of the system is needed for accurate results.

First, the equivalent dc network must be created from the ac power system [5]. As the impedances of each phase of the system are identical – i.e., the phase conductors (transmission lines and transformer windings in each phase) provide identical parallel paths for GIC flows – the calculations of

GICs are performed for a single phase only, and the same result applies to each phase. Each resistive branch is replaced by its corresponding admittance value and voltage sources. Transmission lines with series capacitive compensation are omitted in the dc model as series capacitors block the flow of GIC. Transformers are modeled with their winding resistance to the substation neutral and, in the case of auto-transformers, both series and common windings are represented explicitly.

PMsGMD currently supports “*gywe-gywe*”, “*gywe-delta*”, “*delta-delta*”, and “*gywe-gywe-auto*” transformer winding configurations, where *gywe* stands for grounded-wye. When unknown, this can be estimated:

- generator step-up (abbr. GSU) transformers: *delta-gywe* with delta on low side
- load transformers: *delta-gywe* with delta on high side
- *gywe-gywe-auto*-transformers: connect portions of the transformer grid where voltage ratio  $\leq 3$
- *gywe-gywe* transformers: connect portions of the transformer grid where voltage ratio  $> 3$ .

In practice, actual geo-electric fields vary with geographical locations. Using a common assumption that the North and East components of the geo-electric field are constant in the geographical area of the transmission line [22], [31], [32], the induced voltage  $\mathcal{V}$  is calculated as

$$\mathcal{V} = \mathcal{E}_N L_N + \mathcal{E}_E L_E = |\mathcal{E}|(\sin(\phi)L_N + \cos(\phi)L_E) \quad (1)$$

where  $L_N, L_E, \mathcal{E}_N, \mathcal{E}_E$ , and  $\phi$  are described in Appendix I of [22]. Due to short length,  $\mathcal{V} = 0$  is assumed for transformers.

This formulation assumes that  $\phi$  is measured in counter-clockwise direction from the positive x axis; in geography, it is convention to measure  $\phi$  in clockwise direction from the positive y axis, consequently conversion is necessary sometimes. The substation grounding resistance is often approximated by using nonlinear regression, based on substation size, maximum kV level, and number of incoming lines as predictor variables.

#### D. Transformer Modeling

The formulation presented in [33] contains two equivalent power system models: one for computing the ac power flows and one for computing the GICs; for some formulations, coupling constraints are added to link GICs to the ac power flow model in the form of reactive power losses. The main difference between them occurs in transformer modeling. AC power flow models typically model transformers as a single edge with a voltage transformation (phase shift and tap change). GIC models, on the other hand, require models of transformers that include details of the series and common windings, as well as other transformer components [34].

Effective GIC in the ac network is computed using the following set of equations:

for  $\forall e \in E^\alpha, t \in T$

$$\tilde{I}_e^t = \begin{cases} |I_{eH}^t| & \text{if } e \in E^\Delta \\ \left| \frac{\alpha_e I_{eH}^t + I_{eL}^t}{\alpha_e} \right| & \text{if } e \in E^y \\ \left| \frac{\alpha_e I_{eS}^t + I_{eC}^t}{\alpha_e + 1} \right| & \text{if } e \in E^\infty \\ 0 & \text{otherwise} \end{cases} \quad (2)$$

where Case 1 models a *gywe-delta* GSU transformer (dc equivalent circuit for this case is illustrated in Fig. 1a), Case 2 models a *gywe-gywe* transformer (dc equivalent circuit for this case is illustrated in Fig. 1b), and Case 3 models a *gywe-gywe-auto*-transformer (dc equivalent circuit for this case is illustrated in Fig. 1c).

As [33] notes, most test networks in the literature neglect GSU transformers. GSUs are used to connect the output terminals of generators to the transmission network. The GSUs and the neutral leg ground points they provide are critical when modeling GICs and methods to mitigate the impact of GICs. Consequently, in network models that lack GSU transformers, the model is assumed to include GSU transformers using the method discussed in [33]. Here it is assumed that GSU transformers are *delta-gywe* transformers.

In this paper the model of [33] is adapted to a multi-period dispatch to model the GIC impacts on power systems. The contribution is a model of temperature change over time as a function of changing GIC and ac flows. Instead of the equivalent Norton representation, the simpler Thevenin representation is used as PMs [14] supports series voltage sources. The continuous-time formulation of the transformer hot-spot thermal model is a first order linear dynamic model that is defined in terms of hot-spot temperature rise over top-oil temperature.

Given the active power  $p_{e,ij}^t$  [p.u.] and reactive power  $q_{e,ij}^t$  [p.u.] flowing into the input terminal of the transformer at time  $t$  [min], the apparent power is defined by

$$s_{e,ij}^t = \sqrt{(p_{e,ij}^t)^2 + (q_{e,ij}^t)^2} \quad (3)$$

Fractional loading of the transformer is defined by

$$k_e^t = \frac{s_{e,ij}^t}{s_e} \quad (4)$$

Steady-state top-oil temperature rise  $\delta$  over ambient is then

$$\delta_{eu}^t = \delta_e^r k^2 \quad (5)$$

where  $\delta_e^r$  is the top-oil temperature rise in [°C] at rated apparent power. For a typical transformer,  $\delta_e^r = 75$ [°C] [35].

From [36], the top-oil temperature rise over ambient is

$$\delta_e(t) = \delta_{eu}(1 - e^{-t/\tau_e}) \quad (6)$$

where  $\tau_e$  is the time constant of the top-oil temperature [min]. A typical value is 71 [mins] [35]. By using a bilinear transform, the hot-spot model is reformulated as a difference equation that is suitable for optimization and simulation [37]:

$$\delta_e^t = \frac{1}{1 + \zeta_e}(\delta_{eu}^t + \delta_{eu}^{t-1}) - \frac{1 - \zeta_e}{1 + \zeta_e} \delta_e^{t-1} \quad (7)$$

where  $t$  is the sample index,  $\zeta_e = 2\tau_e/\Delta$  is the discretized time constant, and  $\Delta$  is the sampling period.

The time constants of the hot-spot temperature rise over the top-oil temperature are typically negligible compared to the top-oil temperature dynamics. The absolute value of the transformer hot-spot is

for  $\forall e \in E^\Delta \cup E^y \cup E^\infty, t \in T$

$$\rho_e^t + \delta_e^t + \eta_e^t \quad (8)$$

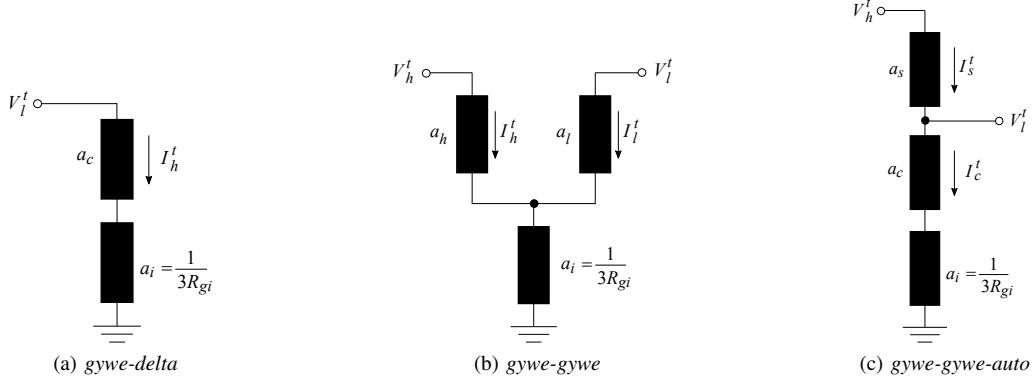


Fig. 1. DC equivalent circuit of different transformer-windings

where  $\rho_e^t$  is the ambient temperature, and assumed to be  $\rho_e^t = 25$  [°C], and  $\eta_e^t$  is the hot-spot temperature rise:

$$\eta_e^t = R_e \tilde{I}_e^t \quad (9)$$

where  $R_e$  is assumed to be  $R_e = 0.63$  [°C/A] and  $\tilde{I}_e^t$  is the transformer effective GIC; i.e. the hot-spot temperature rise is linear with respect to the effective GIC.

### III. STEADY-STATE FORMULATIONS

Before presenting the time-extended formulation, first the common industry and academic steady-state formulations implemented in PMsGMD are discussed.

#### 1) GIC DC: quasi-dc power flow.

Solves steady-state dc currents on lines resulting from induced dc voltages on lines.

#### 2) GIC $\rightarrow$ AC – OPF: sequential quasi-dc power flow and optimal power flow.

Solves for quasi-dc voltages and currents, and uses the calculated quasi-dc currents through transformer windings as inputs to an AC-OPF in order to calculate the increase in transformer reactive power consumption.

#### 3) GIC + AC – OPF: ac optimal power flow coupled with a quasi-dc power flow.

Solves for quasi-dc voltages and currents, and solves the AC-OPF concurrently. The dc network couples to the ac network by means of reactive power loss in transformers. This formulation does not model increases in transformer reactive power consumption caused by changes in the ac terminal voltages. Additionally, it may report higher reactive power consumption than reality as it relaxes the “effective” transformer quasi-dc winding current magnitude.

#### 4) GIC + AC – MLS: ac minimum-load-shed coupled with a quasi-dc power flow.

Solves the minimum-load shedding problem for a network subjected to GIC with fixed topology. It uses load shedding to protect the system from GIC-induced voltage collapse and transformer over-heating.

#### 5) GIC + AC – OTS: ac optimal transmission switching with load shed coupled with a quasi-dc power flow.

Solves the minimum-load shedding problem for a network subjected to GIC, where lines and transformers can be opened or closed. It uses transmission-switching to protect the system from GIC-induced voltage collapse and transformer over-heating.

### IV. TIME-SERIES EXTENSION OF THE AC-OTS PROBLEM SPECIFICATION

Below the problem specification for the AC-OTS use case of PMsGMD is described. This problem uses the top-oil temperature dynamics described in Section II to link time-periods. Line switching configurations are shared across all time-periods. In this paper the dc power flow approximation of the full ac non-convex power flow constraints is used to ease computational burden. However, switching to the full set of ac power flow constraints or relaxations is seamless given the PMs framework.

#### 1) Objective function:

$$\min \sum_{g \in G, t \in T} \kappa_g^0 + \kappa_g^1 p_g^t + \kappa_g^2 (p_g^t)^2 \quad (10)$$

#### 2) DC power flow approximation equations:

for  $\forall i \in N^a, t \in T$

$$\sum_{e \in E_i^+} p_{e,ij}^t - \sum_{e \in E_i^-} p_{e,ij}^t = \sum_{g \in G_i} p_g^t - p_i^t - g_i \quad (11)$$

for  $\forall e \in E^a, t \in T$

$$p_{e,ij}^t = z_e b_e (\theta_i^t - \theta_j^t) \quad (12a)$$

$$p_{e,ji}^t = -p_{e,ij}^t \quad (12b)$$

#### 3) Operational limit constraints:

for  $\forall e \in E^a, t \in T$

$$p_{e,ij}^t \leq z_e \bar{s}_e \quad (13a)$$

$$p_{e,ji}^t \leq z_e \bar{s}_e \quad (13b)$$

$$|\theta_i^t - \theta_j^t| \leq z_e \bar{\theta} + (1 - z_e) \theta^M \quad (13c)$$

for  $\forall g \in G, t \in T$

$$\underline{p}_g \leq p_g^t \leq \bar{p}_g \quad (14)$$

4) *GIC effects on transformers:*

for  $\forall i \in N^d$

$$\sum_{e \in E_i^+} I_e^t - \sum_{e \in E_i^-} I_e^t = a_i V_i^d \quad (15)$$

for  $\forall e \in \mathcal{E}^d, t \in T$

$$I_e^t = z_{\vec{e}} a_e (V_i^t - V_j^t + \mathcal{V}_e^t) \quad (16)$$

for  $\forall e \in E^a, t \in T$

$$\tilde{I}_e^t \geq +/ - \begin{cases} I_{eH}^t & \text{if } e \in E^\Delta \\ \frac{\alpha_e I_{eH}^t + I_{eL}^t}{\alpha_e} & \text{if } e \in E^y \\ \frac{\alpha_e I_{eS}^t + I_{eC}^t}{\alpha_e + 1} & \text{if } e \in E^\infty \\ 0 & \text{otherwise} \end{cases} \quad (17)$$

for  $\forall e \in \mathcal{E}^\tau$

$$0 \leq \tilde{I}_e^d \leq \bar{I}_e^d \quad (18)$$

$$\text{Eq. (7), (9)} \quad (19)$$

for  $\forall e \in E^\Delta \cup E^y \cup E^\infty, t \in T$

$$\rho_e^t + \delta_e^t + \eta_e^t \leq \mathcal{T}_e \quad (20)$$

for  $\forall e \in \mathcal{E}^a, g \in G$

$$z_e \in \{0, 1\} \quad (21)$$

5) *Supporting constraints:*

for  $\forall e \in E^a, t \in T$

$$\tilde{I}_e^t \leq z_e \bar{I}_e^d \quad (22)$$

The objective function (10) minimizes total generator dispatch costs and load shedding costs. Constraints (11)-(12) describe the dc power flow physics and engineering constraints associated with a power system. Constraint (11) models power balance at each node (Kirchoff's Law). Constraints (12a) and (12b) model the dc approximation of ac power flow on each transmission line with on-off variables  $z_e$  (Ohm's Law)..

Constraints (13)-(14) describe the operational limits of the power system. Constraints (13a) and (13b) model the thermal limits of lines in both directions. Constraint (13c) applies bounds on the phase angle difference between two buses. Constraint (14) models the capacity of power generation. The dc circuit and effects associated with the GMD are formulated in constraints (15)-(21). An edge ( $e \in \mathcal{E}^d$ ) in the dc circuit is linked to an edge in the ac circuit ( $\vec{e}$ ). Constraints (15) and (16) formulate the GIC flow on each dc line by applying Kirchoff's current law using the Thevenin representation.

The GIC on a line is determined by the induced current source and the quasi-dc voltage difference between two buses [22]. GIC flow is forced to 0 by  $z_{\vec{e}}$  when  $\vec{e}$  is switched off. Constraint (17) computes the effective (non-negative) GIC on each ac edge by relaxing the absolute values in (2) with two inequalities. The effective GIC is calculated at the time scale of the ac circuit. Constraint (18) models the maximum

allowed value of GIC flowing through a transformer for safe operation. Constraint (19) computes the ac and GIC hot-spot heating temperature at every time step using Equations (7) and (9). Constraint (20) forces transformer temperatures below a thermal limit. Finally, constraint (22) explicitly forces the effective GIC to 0 when an edge is inactive.

Code Block 1 (on Page 7) shows how this specification is implemented in PMsGMD in Julia. Some function names are abbreviated due to space constraints.

## V. CASE STUDY

To demonstrate the application and performance of PMs-GMD, in addition validate the implementation of the AC-OTS "ac optimal transmission switching with load shed coupled with a quasi-dc power flow" problem specification (presented in Section IV), a GMD case study is carried out. The hypothetical network designed by Horton et al. [31] for GIC modeling software validation is used. This 21-bus extra high voltage power system model – depicted in Figs. 2 and 3 – consists of 345 [kV] and 500 [kV] lines and transformers, and is centered over the State of Tennessee, USA. The model includes single transmission lines as well as some that occupy the same transmission corridor; the substations feature both conventional and auto-transformers, furthermore, series and neutral connected GIC blocking devices are also included.

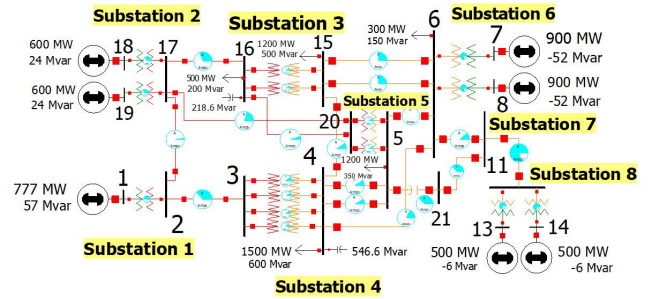


Fig. 2. One-line diagram of the used case study system

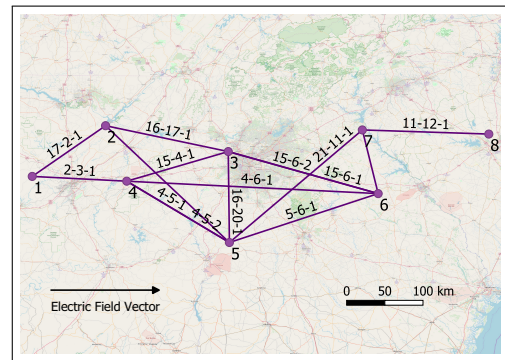


Fig. 3. Map of the used case study system and electric field vector

The Horton case study system provides all parameters necessary for calculations of GICs, including bus-substation connectivity and substation geographical locations. In order

---

**Code Block 1** Coupled Quasi-DC and AC-OTS Model
 

---

```

function post_gmd_ots_ts(pm::GenericPowerModel)
  for (n, network) in nws(pm)
    PMs.variable_vol_on_off(pm, nw=n)
    PMs.variable_generation(pm, nw=n)
    PMs.variable_branch_flow(pm, nw=n)

    PMs.variable_branch_indicator(pm, nw=n)

    PG.variable_dc_current_mag(pm, nw=n)
    PG.variable_dc_current(pm, nw=n)
    PG.variable_dc_line_flow(pm; bounded=false, nw=n)
    PG.variable_dc_volt_on_off(pm, nw=n)
    PG.variable_reactive_power_loss(pm, nw=n)

    variable_delta_oil_ss(pm, nw=n)
    variable_delta_oil(pm, nw=n)
    variable_delta_hotspot_ss(pm, nw=n)
    variable_delta_hotspot(pm, nw=n)
    variable_hotspot(pm, nw=n)

    PMs.cons_model_volt_on_off(pm, nw=n)

    for i in PMs.ids(pm, :ref_buses, nw=n)
      PMs.cons_theta_ref(pm, i, nw=n)
    end

    for i in PMs.ids(pm, :bus, nw=n)
      PG.cons_kcl_gmd(pm, i, nw=n)
    end

    for i in PMs.ids(pm, :branch, nw=n)
      PG.cons_dc_current_mag_on_off(pm, i, nw=n)
      PG.cons_qloss_vnom(pm, i, nw=n)

      PMs.cons_ohms_yt_from_on_off(pm, i, nw=n)
      PMs.cons_ohms_yt_to_on_off(pm, i, nw=n)

      PMs.cons_volt_angle_diff_on_off(pm, i, nw=n)

      PMs.cons_thermal_lim_from_on_off(pm, i, nw=n)
      PMs.cons_thermal_lim_to_on_off(pm, i, nw=n)

      cons_temperature_ss(pm, i, nw=n)
      cons_hotspot_temp_ss(pm, i, nw=n)
      cons_hotspot_temp(pm, i, nw=n)
      cons_absolute_hotspot_temp(pm, i, nw=n)
    end

    for i in PMs.ids(pm, :gmd_bus)
      PG.cons_dc_kcl_shunt(pm, i, nw=n)
    end

    for i in PMs.ids(pm, :gmd_branch)
      PG.cons_dc_ohms_on_off(pm, i, nw=n)
    end
  end

  network_ids = sort(collect(nw_ids(pm)))

  n_1 = network_ids[1]
  for i in ids(pm, :branch, nw=n_1)
    cons_temperature_state(pm, i, nw=n_1)
  end

  for n_2 in network_ids[2:end]
    for i in ids(pm, :branch, nw=n_2)
      cons_temperature_state(pm, i, n_1, n_2)
    end
    n_1 = n_2
  end

  PMs.objective_min_fuel_and_flow_cost(pm)
end

```

---

to simulate a realistic system operation scenario, a number of lines are disconnected (as indicated in the above figures) assuming planned system-maintenance and unforeseen outages due to a GMD event; consequently, the size of the network is reduced to 11 buses. Table VI summarizes these initial assumptions for each branch.

TABLE VI  
BRANCH STATUSES IN THE CASE STUDY SYSTEM

$i$	$j$	$Ckt.$	$Type$	$z_e^{nom}$	$z_e$	$p_{e,ij}$	$I_e$
1	2	1	xf	1	1	8.3	0.0
2	3	1	line	1	1	8.3	0.0
3	4	1	xf	1	1	2.1	-56.6
3	4	2	xf	1	1	2.1	-56.6
3	4	3	xf	1	1	2.1	127.8
3	4	4	xf	1	1	2.1	127.8
4	5	1	line	1	1	-6.7	368.8
4	5	2	line	1	0	0.0	0.0
4	6	1	line	1	0	0.0	0.0
5	6	1	line	1	1	-18.7	368.8
5	20	1	xf	0	0	0.0	0.0
5	20	2	xf	0	0	0.0	0.0
5	21	1	series_cap	0	0	0.0	0.0
6	7	1	xf	1	1	-8.3	21.5
6	8	1	xf	1	1	-8.3	21.5
6	11	1	line	1	1	-5.0	325.9
11	12	1	line	1	1	-5.0	325.9
12	13	1	xf	1	1	-5.0	325.9
12	14	1	xf	0	0	0.0	0.0
15	4	1	line	0	0	0.0	0.0
15	6	1	line	0	0	0.0	0.0
15	6	2	line	0	0	0.0	0.0
16	15	1	xf	0	0	0.0	0.0
16	15	2	xf	0	0	0.0	0.0
16	17	1	line	0	0	0.0	0.0
16	20	1	line	0	0	0.0	0.0
17	2	1	line	0	0	0.0	0.0
17	18	1	xf	0	0	0.0	0.0
17	19	1	xf	0	0	0.0	0.0
17	20	1	line	0	0	0.0	0.0
21	11	1	line	0	0	0.0	0.0

The system is subjected to a time-varying uniform East-West electric field (as indicated in Fig. 3), which varies linearly from 0 V/km to 3.2 V/km over the first 3 hours and then back down linearly to 0 V/km over the remaining 3 hours of the simulation, illustrated in Fig. 4.

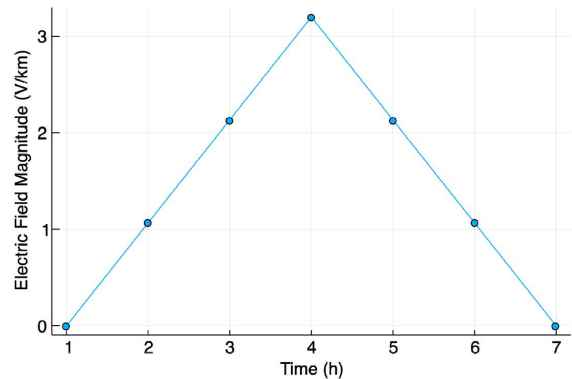


Fig. 4. Time variation of the electric field magnitude

## VI. EVALUATION OF RESULTS

The simulation was performed on a computer with a quad-core Intel® Core™ i5-6500 3.2GHz CPU, and 8GB RAM. The used software was Julia v1.0 [13], using Gurobi v8.1 [17] for MacOS as nonlinear solver.

Parts of the results are presented in Table VI: the columns  $z_e^{nom}$  and  $z_e$  list the nominal branch statuses along with the branch statuses produced by the optimizer, respectively. The mitigation strategy determination takes 21 [sec]. The optimizer chooses to relieve GIC flowing through the transformers at Substations 1, 4 and 6; it accomplishes this by opening the longest predominantly East-West directional line 4-6-1, along with one of the lines in the 4-5 transmission corridor.

Fig. 5 illustrates the temperature of transformer 12-13-1, located at substation 8 of Fig. 3; the designed mitigation strategy kept its temperature below the instantaneous limit of 280°C. This admittedly high instantaneous limit is selected with a bias to supplying load power at the cost of significant loss-of-life to transformer insulation; nevertheless, this limit can be adjusted as needed.

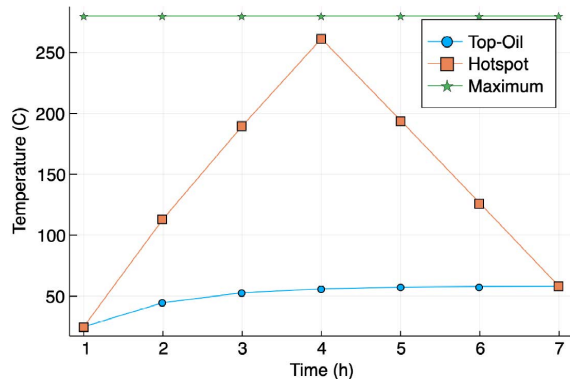


Fig. 5. Hot-spot temperature for transformer 12-13-1

## VII. CONCLUSION

As the threat of GMD and E3 HEMP events continues to pose a substantial risk to our energy infrastructures, accurate simulation and effective mitigation becomes increasingly important. This paper presented an extensible open-source modeling framework for both analyzing and optimally mitigating the impacts of such hazards.

By design, PMSGMD is suitable to monitor disturbance-manifestations in real-time and predict GICs on the electrical grid. In addition, by extending PMSGMD with the problem of mitigating transformer heating by switching lines given a time-varying electric field, along with techniques to improve the scalability of the problem, a GIC mitigation capability is enabled; providing mitigation-strategies in a reasonable amount of time demonstrates the utility of this modular framework.

The performed case study validates implementation and demonstrates performance; further simulations on larger size networks are future tasks. Other extensions to the presented GIC power flow problem are possible under the PMSGMD framework, such as optimal GIC blocker placement, harmonic load flow, and scenario-based problem formulations.

**Acknowledgements** This work was supported by the U.S. DOE LDRD Program at Los Alamos National Laboratory under the “Impacts of Extreme Space Weather Events on Power Grid Infrastructure: Physics-Based Modelling of Geomagnetically-Induced Currents (GICs) During Carrington-Class Geomagnetic Storms” project.

## REFERENCES

- [1] NERC and U.S. Department of Energy. High-Impact, Low-Frequency Event Risk to the North American Bulk Power System. Technical report, North American Electric Reliability Corporation, Jun. 2010.
- [2] DHS Cybersecurity & Infrastructure Security Agency. Homeland Security Presidential Directive 7. Technical report, U.S. Department of Homeland Security, Dec. 2003.
- [3] V. D. Albertson, J. M. Thorson, R. E. Clayton, and S. C. Tripathy. Solar-Induced-Currents in Power Systems: Cause and Effects. *IEEE Transactions on Power Apparatus and Systems*, PAS-92(2):471–477, Mar. 1973.
- [4] A. Mate. *A Generation Prioritization Method for Power System Restoration with Renewable Resources*. PhD thesis, Oregon State University, Jun. 2020.
- [5] D. H. Boteler and R. J. Pirjola. Modeling Geomagnetically Induced Currents. *Space Weather*, 15(1):258–276, Jan. 2017.
- [6] T. R. Hutchins and T. J. Overbye. Power System Dynamic Performance During the Late-Time (E3) High-Altitude Electromagnetic Pulse. In *Proceedings of the 2016 Power Systems Computation Conference*, pages 1–6, Jun. 2016.
- [7] R. Pirjola. Geomagnetically Induced Currents During Magnetic Storms. *IEEE Transactions on Plasma Science*, 28(6):1867–1873, Dec. 2000.
- [8] T. R. Hutchins and T. J. Overbye. The Effect of Geomagnetic Disturbances on the Electric Grid and Appropriate Mitigation Strategies. In *Proceedings to the 2011 North American Power Symposium*, pages 1–5, Aug. 2011.
- [9] J. Berge and R. K. Varma. Modeling and Mitigation of Geomagnetically Induced Currents on a Realistic Power System Network. In *Proceedings to the 2011 IEEE Electrical Power and Energy Conference*, pages 485–490, Oct 2011.
- [10] T. J. Overbye, K. S. Shetye, T. R. Hutchins, Q. Qiu, and J. D. Weber. Power Grid Sensitivity Analysis of Geomagnetically Induced Currents. *IEEE Transactions on Power Systems*, 28(4):4821–4828, Nov. 2013.
- [11] NERC. Effects of Geomagnetic Disturbances on the Bulk Power System System. Technical report, North American Electric Reliability Corporation, Feb. 2012.
- [12] K. S. Shetye and T. J. Overbye. Modeling and Analysis of GMD Effects on Power Systems: An Overview of the Impact on Large-Scale Power Systems. *IEEE Electrification Magazine*, 3(4):13–21, Dec. 2015.
- [13] J. Bezanson, S. Karpinski, V. B. Shah, and A. Edelman. Julia: A Fast Dynamic Language for Technical Computing. <https://julialang.org>, 2012.
- [14] C. Coffrin, R. Bent, K. Sundar, Y. Ng, and M. Lubin. PowerModels.jl: An Open-Source Framework for Exploring Power Flow Formulations. In *Proceedings of the 2018 Power Systems Computation Conference*, pages 1–8, June 2018.
- [15] I. Dunning, J. Huchette, and M. Lubin. JuMP: A Modeling Language for Mathematical Optimization. *SIAM Review*, 59(2):295–320, 2017.
- [16] A. Wachter and L. T. Biegler. On the Implementation of a Primal-Dual Interior Point Filter Line Search Algorithm for Large-Scale Nonlinear Programming. *Mathematical Programming*, 106(1):25–57, Mar. 2006.
- [17] Gurobi Optimization LLC. Gurobi Optimizer Reference Manual. <http://www.gurobi.com>, 2019.
- [18] IBM Corp. CPLEX User’s Manual. <https://www.ibm.com>, 2019.
- [19] R. D. Zimmerman, C. E. Murillo-Sánchez, and R. J. Thomas. MATPOWER: Steady-State Operations, Planning and Analysis Tools for Power Systems Research and Education. *IEEE Transactions on Power Systems*, 26(1):12–19, Feb. 2011.
- [20] T. R. Hutchins and T. J. Overbye. Power Flow Studies in the Presence of Geomagnetically Induced Currents. In *Proceedings of the 2012 IEEE Power and Energy Conference at Illinois*, pages 1–4, Feb. 2012.
- [21] T. J. Overbye, T. R. Hutchins, K. S. Shetye, J. D. Weber, and S. Dahman. Integration of Geomagnetic Disturbance Modeling Into the Power Flow: A Methodology for Large-Scale System Studies. In *Proceedings of the 2012 North American Power Symposium*, pages 1–7, Sep. 2012.
- [22] NERC Application Guide. Computing Geomagnetically-Induced Current in the Bulk-Power System. Technical report, North American Electric Reliability Corporation, Dec. 2013.



- [23] M. Kazerooni, H. Zhu, T. J. Overbye, and D. A. Wojtczak. Transmission System Geomagnetically Induced Current Model Validation. *IEEE Transactions on Power Systems*, 32(3):2183–2192, May. 2017.
- [24] C. Klauber, G. P. Juvekar, K. Davis, T. Overbye, and K. Shetye. The Potential for a GIC-inclusive State Estimator. In *Proceedings of the 2018 North American Power Symposium*, pages 1–6, Sep. 2018.
- [25] G. P. Juvekar and K. Davis. MATGMD: A Tool for Enabling GMD Studies in MATLAB. In *Proceedings of the 2019 IEEE Texas Power and Energy Conference*, pages 1–6, Feb. 2019.
- [26] PowerWorld Corporation. PowerWorld® Simulator. <https://www.powerworld.com>, 2019.
- [27] Siemens. PSS®E. <https://new.siemens.com>, 2019.
- [28] A. Schultz, S. Murphy, E. Cotilla-Sanchez, N. Imamura, A. Mate, and A. Barnes. Fusing Magnetotelluric, Magnetic Observatory and Power Grid Sensor Data with Real-Time Power Flow Analysis: Providing Actionable Information to Mitigate Risk to the Power Grid from Geomagnetic Disturbances/EMP. In *Technical Presentation at the American Geophysical Union 2019 Fall Meeting*, Dec. 2019.
- [29] M. Lu, S. D. Eksioğlu, S. J. Mason, R. Bent, and H. Nagarajan. Distributionally Robust Optimization for a Resilient Transmission Grid During Geomagnetic Disturbances. <https://arxiv.org/abs/1906.04139>, 2019.
- [30] S. Dahman. Geomagnetically Induced Current (GIC) Modeling. In *Proceedings of the 2016 PowerWorld Client Conference*, Feb. 2016.
- [31] R. Horton, D. Boteler, T. J. Overbye, R. Pirjola, and R. C. Dugan. A Test Case for the Calculation of Geomagnetically Induced Currents. *IEEE Transactions on Power Delivery*, 27(4):2368–2373, Oct. 2012.
- [32] H. Zhu and T. J. Overbye. Blocking Device Placement for Mitigating the Effects of Geomagnetically Induced Currents. *IEEE Transactions on Power Systems*, 30(4):2081–2089, Jul. 2015.
- [33] M. Lu, H. Nagarajan, E. Yamangil, R. Bent, S. Backhaus, and A. Barnes. Optimal Transmission Line Switching Under Geomagnetic Disturbances. *IEEE Transactions on Power Systems*, 33(3):2539–2550, May 2018.
- [34] K. Zheng, D. Boteler, R. J. Pirjola, L.-G. Liu, R. Becker, L. Marti, S. Boutilier, and S. Guillon. Effects of System Characteristics on Geomagnetically Induced Currents. *IEEE Transactions on Power Delivery*, 29(2):890–898, Apr. 2014.
- [35] D. Susa, M. Lehtonen, and H. Nordman. Dynamic Thermal Modelling of Power Transformers. *IEEE Transactions on Power Delivery*, 20(1):197–204, Jan. 2005.
- [36] X. Mao, D. J. Tylavsky, and G. A. McCulla. Dynamic Thermal Modelling of Power Transformers. *IEEE Proceedings on Generation, Transmission and Distribution*, 153(4):414–422, Jul. 2006.
- [37] R. Hurton. Magnetohydrodynamic Electromagnetic Pulse Assessment of the Continental U.S. Electric Grid. Technical report, Electric Power Research Institute, Feb. 2017.

## NOMENCLATURE

### Sets

- $E^a$  set of directed edges in the ac circuit, indexed by  $e$
- $E^d$  set of directed edges in the dc circuit, indexed by  $e$  and oriented from dc bus  $i$  to dc bus  $j$
- $E^y \subseteq E^a$  set of gwyne-gwyne transformers in the ac circuit, indexed by  $e$
- $E^\Delta \subseteq E^a$  set of delta-gwyne transformers in the ac circuit, indexed by  $e$
- $E_i^- \subseteq E^a \cup E^d$  set of directed edges connected to node  $i$ , indexed by  $e$ , that are oriented from  $j$  to  $i$
- $E^\infty \subseteq E^a$  set of auto gwyne-gwyne transformers in the ac circuit, indexed by  $e$  and oriented from bus  $i$  to bus  $j$
- $G$  set of generators in the ac circuit, indexed by  $g$
- $G_i$  set of generators in the ac circuit connected to bus  $i \in N^a$ , indexed by  $g$
- $N^a$  set of nodes (buses) in the ac circuit, indexed by  $i$
- $N^d$  set of nodes (buses) in the dc circuit, indexed by  $i$
- $N_l^a \subseteq N^a$  set of nodes with ac load
- $T$  set of time periods, indexed by  $t$ , numbered from  $0 \dots |T|$

### Parameters

- $a_e$  dc admittance of edge  $e \in E^d$
- $a_i$  admittance of the grounding line at dc bus  $i \in N^d$ , 0 if the bus is not the substation neutral
- $e^H, e^L, e^S, e^C \in E^d$  high side, low side, series, and common winding dc edges for  $e \in E^\Delta \cup E^y \cup E^\infty$ , respectively
- $\vec{e}$  ac edge associated with dc edge  $e \in E^d$
- $g_i$  shunt conductance at bus  $i \in N^a$
- $\bar{I}_e^d$  maximum dc current on line  $e \in E^a$
- $L_N, L_E$  the north and east components of the displacement of each transmission line, respectively
- $n_e$  top-oil cooling factor for  $e \in E^\Delta \cup E^y \cup E^\infty$
- $p_i^t$  real power demand at bus  $i \in N^a$  at time  $t \in T$
- $\underline{p}_g$  minimum real power generation at generator  $g \in G$
- $\bar{p}_g$  maximum real power generation at generator  $g \in G$
- $R_e$  thermal hot-spot resistance for  $e \in E^\Delta \cup E^y \cup E^\infty$
- $\bar{s}_e$  apparent power limit on line  $e \in E^a$
- $\mathcal{V}_e^t$  GMD induced voltage source at time  $t \in T$
- $x_e$  reactance of line  $e \in E^a$
- $\alpha_e$  turns ratio for  $e \in E^\Delta \cup E^y \cup E^\infty$
- $\delta_e^r$  top-oil temperature rise in  $^\circ\text{C}$  at rated apparent power for  $e \in E^\Delta \cup E^y \cup E^\infty$
- $\Delta$  duration of a time period
- $\mathcal{E}_N, \mathcal{E}_E$  strength of the north and east geo-electric field at time  $t \in T$ , respectively
- $\zeta_e$  discretized top-oil temperature time constant of  $e \in E^\Delta \cup E^y \cup E^\infty$
- $\theta^M$  big-M parameter given by  $|E^a| \bar{\theta}$
- $\bar{\theta}$  phase angle difference limit
- $\kappa_g^0, \kappa_g^1, \kappa_g^2$  generation cost coefficients of generator  $g \in G$
- $\rho_e^t$  ambient temperature at transformer edge  $e \in E^\Delta \cup E^y \cup E^\infty$  at time  $t \in T$
- $\tau_e$  top-oil temperature time constant of  $e \in E^\Delta \cup E^y \cup E^\infty$
- $\mathcal{T}_e$  maximum temperature of  $e \in E^\Delta \cup E^y \cup E^\infty$
- $\phi^t$  the angle of the geo-electric field relative to east at time  $t \in T$

### Variables

- $I_e^t$  GIC flow on dc line  $e \in E^d$  at time  $t \in T$
- $\tilde{I}_e^t$  the effective GIC on line  $e \in E^a$  at time  $t \in T$
- $p_{e,ij}^t$  real power flow on line  $e \in E^a$ , as measured at node  $i$  at time  $t \in T$
- $p_{e,ji}^t$  real power flow on line  $e \in E^a$ , as measured at node  $j$  at time  $t \in T$
- $p_g^t$  real and reactive power generated at generator  $g \in G$  at time  $t \in T$
- $q_{e,ij}^t$  reactive power flow on line  $e \in E^a$ , as measured at node  $i$  at time  $t \in T$
- $s_{e,ij}^t$  apparent power flow on line  $e \in E^a$ , as measured at node  $i$  at time  $t \in T$
- $V_i^t$  induced dc voltage magnitude at bus  $i \in N^d$  at time  $t \in T$
- $z_e$  1 if line  $e \in E^a$  is switched on; 0 otherwise
- $\delta_e^t$  top oil temperature at transformer edge  $e \in E^\Delta \cup E^y \cup E^\infty$  at time  $t \in T$